ACS Macro Letters

Letter

pubs.acs.org/macroletters

Writing Highly Ordered Macroscopic Patterns in Cylindrical Block Polymer Thin Films via Raster Solvent Vapor Annealing and Soft Shear

Ming Luo,[†] Douglas M. Scott,[†] and Thomas H. Epps, III*[,†,‡]

[†]Department of Chemical and Biomolecular Engineering and [‡]Department of Materials Science and Engineering, University of Delaware, Newark, Delaware 19716, United States

Supporting Information

ABSTRACT: Block polymers (BPs) potentially can be used to template large arrays of nanopatterns for advanced nanotechnologies. However, the practical utilization of directed BP self-assembly typically requires guide patterns of relatively small size scales. In this work, the macroscopic alignment of block polymer cylinders on a template-free substrate is achieved through raster solvent vapor annealing combined with soft shear (RSVA-SS). Spatial control over nanoscale structures is realized by using a solvent vapor delivery nozzle, poly(dimethylsiloxane) shearing pad, and motorized stage. Complex patterns including dashes, crossed lines, and curves are demonstrated, along with the ability for large area alignment and scale-up for industry applications. The unique ability to directly write macroscopic patterns with microscopically aligned BP nanostructures will open new avenues of applied research in nanotechnology.

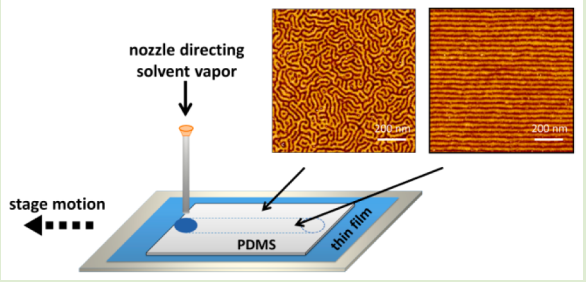

The macroscopic alignment of nanoscale periodic structures in block polymer (BP) thin films is attracting increased attention due to its necessity for unlocking various applications in materials chemistry and nanotechnology.[1−7] For example, spherical or cylindrical nanostructures formed by self-assembled BPs have been used successfully to pattern semiconductors, fabricate ultradense arrays of metal nanowires, and template magnetic storage media;[8−13] however, progress in the widespread adoption of BPs for these applications has been impeded by the lack of a versatile and efficient technique for inducing the long-range order and orientation of nanostructures in a predetermined direction. One major difficulty is that BPs tend to self-assemble in an isotropic manner in the absence of surface forces and external fields.[14−16] Thus, many techniques have been developed to guide BP self-assembly with varying degrees of success. Graphoepitaxy creates single-crystalline ordered structures, but the required substrate prepatterning can limit the size of the arrays that can be fabricated.[17,18] Additionally, valuable substrate area is lost due to patterning. Chemical prepatterning can direct BP alignment over large areas, but it requires substrate modification at the nanometer scale; this process can be prohibitively slow.[19,20] Electric fields, magnetic fields, and polarized light also have been explored but are limited to specialized polymer systems.[21−23] To address these above limitations, researchers are actively developing new and more universal methods to efficiently direct BP self-assembly on template-free substrates through cost-effective means.

Shear fields are an established approach to align BPs in bulk[24,25] and have been employed to align single-layer BP thin films (~30 nm) as demonstrated by Register and Chaikin.[26,27] In these works, shear stress was applied by the deformation and displacement of a cross-linked poly(dimethylsiloxane) (PDMS) pad placed on top of a cylinder-forming BP thin film, and the BP domain orientation was correlated strongly with the shear direction after thermal annealing under shear for an hour.[26] This technique could be modified easily for larger or smaller areas by changing the size of the elastomer pad. However, the alignment quality degraded quickly as the BP film thickness deviated from a single domain spacing.[26] Additionally, the time scale of this processing method may not be ideal for alignment in all applications.

Recently, other techniques have been combined with shear fields to facilitate alignment in BP thin films.[28−30] Karim et al. employed a moving temperature gradient in conjunction with shear, termed cold zone annealing-soft shear (CZA-SS).[28] In the case of CZA-SS, an elastomeric PDMS layer was placed on top of the BP film and undergoes directional expansion and contraction due to a dynamic thermal field, thereby imposing an oscillatory shear field on the underlying BP film. Using this process, horizontally aligned BP cylinders were fabricated continuously in films over a wide thickness range of 40−1000 nm at an industrially relevant speed of v = 12 mm/min (i.e., 200 μm/s). However, this process required high annealing temperatures, well above the glass transition temperature (T_g) of the BP to enable chain mobility, and only was applicable to

Received: February 16, 2015
Accepted: April 14, 2015
Published: April 20, 2015

DOI: 10.1021/acsmacrolett.5b00126
ACS Macro Lett. 2015, 4, 516−520

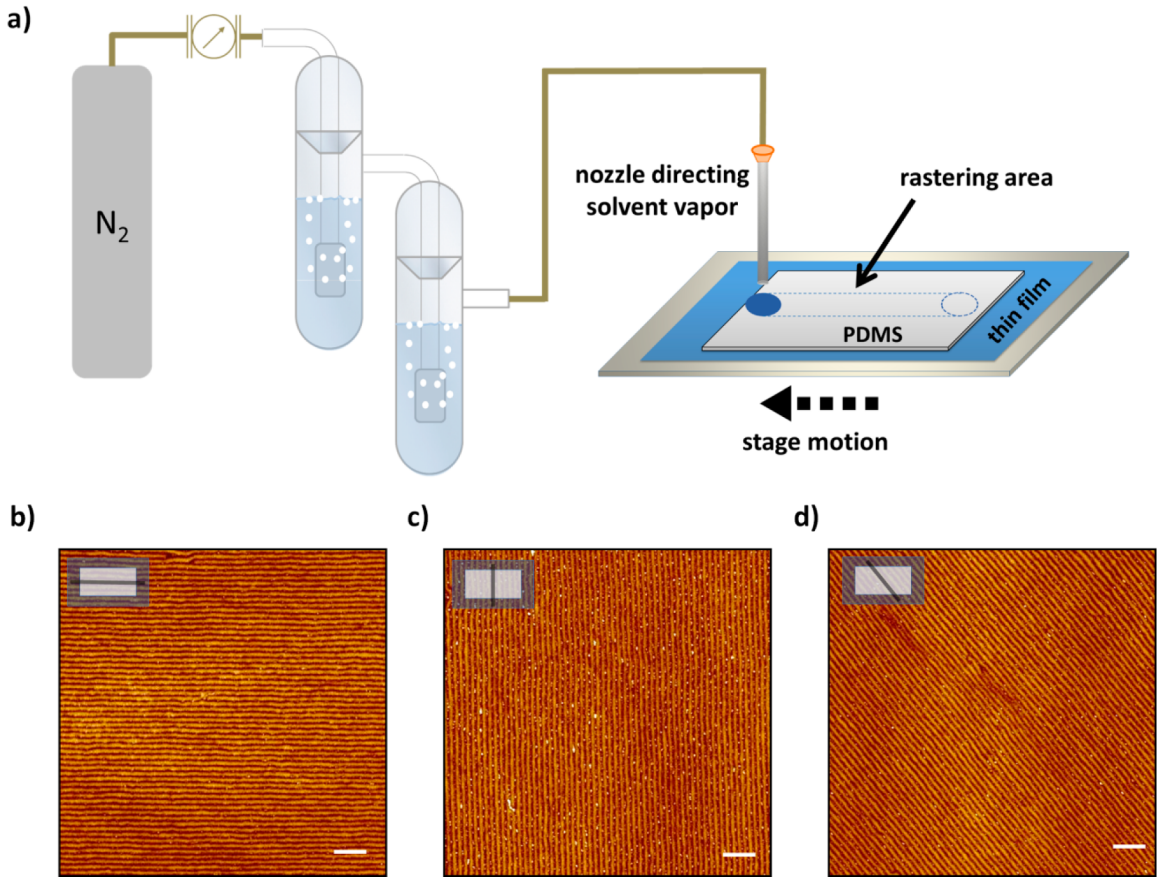

Figure 1. (a) Schematic of RSVA-SS process. (b), (c), and (d) AFM phase images of the SIS thin films treated with RSVA-SS, demonstrating in-plane horizontal, vertical, and diagonal alignment of SIS cylinders. The orientation of the SIS cylinders correlated strongly with the rastering path as indicated in the inset. Scale bars represent 200 nm.

BPs with an accessible $T_g \ll T_{ODT}$ (order−disorder transition temperature). More recently, Jung and co-workers demonstrated that unidirectional alignment of BP cylinders could be produced by solvent vapor annealing (SVA) partnered with shear.[31] A solvent-containing PDMS pad was placed on top of a BP film, and shear alignment was accomplished by the movement of the PDMS pad across the film surface. The solvent vapor effectively decreases the T_g of the BP and imparts mobility to the polymer chains, thus making this approach readily applicable to a vast array of BPs.[32] Cavicchi, Vogt, and co-workers further showed alignment of BP thin films using a flow chamber annealing method (solvent flow in/out of a chamber).[29,33,34] The nanostructure alignment was found to be induced primarily by contraction of the PDMS pad during solvent removal. However, the resulting alignment depended strongly on the shape and placement of the PDMS pad, and this method is not directly amenable to continuous processing.

Our present study demonstrates a simple but effective method to achieve macroscopic alignment of BP cylinders through the application of raster solvent vapor annealing with soft shear (RSVA-SS). This method significantly improves on previous approaches by eliminating the correlation between the BP alignment and PDMS shape, allowing continuous fabrication of highly ordered BP cylinder patterns in a two-dimensional manner. This advance makes the RSVA-SS approach more attractive for the industrial production of hierarchically patterned BP nanostructures. Spatial control over nanoscale structures was accomplished through the implementation of a solvent vapor delivery nozzle and motorized stage. In this manner, macroscopic patterns of nanoscale features could be "written" in a controlled fashion into the BP thin film. We demonstrate that complex patterns such as dashes, crossed lines, and curves can be imparted easily to thin films on featureless and untreated substrates. Additionally, the capability to erase and rewrite the patterns affords advantages over conventional patterning methods. Furthermore, the ability to expand or shrink the "writing" size of the oriented regions from millimeters to centimeters (decoupled from the size of the PDMS pad) provides a unique handle for manipulating pattern formation in an on-demand fashion. Finally, the RSVA-SS approach provides a feasible and scalable pathway for the continuous processing of various copolymer systems, especially those containing thermally sensitive or thermally responsive components.

A schematic of RSVA-SS is shown in Figure 1a. In this case, a thin film of cylinder-forming poly(styrene-*b*-isoprene-*b*-styrene) (SIS) was flow coated onto an UV-ozone cleaned silicon substrate (SIS film was ≈90 nm thick), and an unpatterned elastomer pad (PDMS) was laminated onto the SIS film. Then, toluene vapor was directed onto the film using a nozzle (for example a ∼0.5 mm in diameter circular nozzle was used in one iteration). The rastering speed and position were controlled by a programmable motorized stage. The elastomeric capping layer was removed easily after RSVA without damaging the BP film. Nanostructure formation and orientation was assessed by atomic force microscopy (AFM).

DOI: 10.1021/acsmacrolett.5b00126
ACS Macro Lett. 2015, 4, 516−520

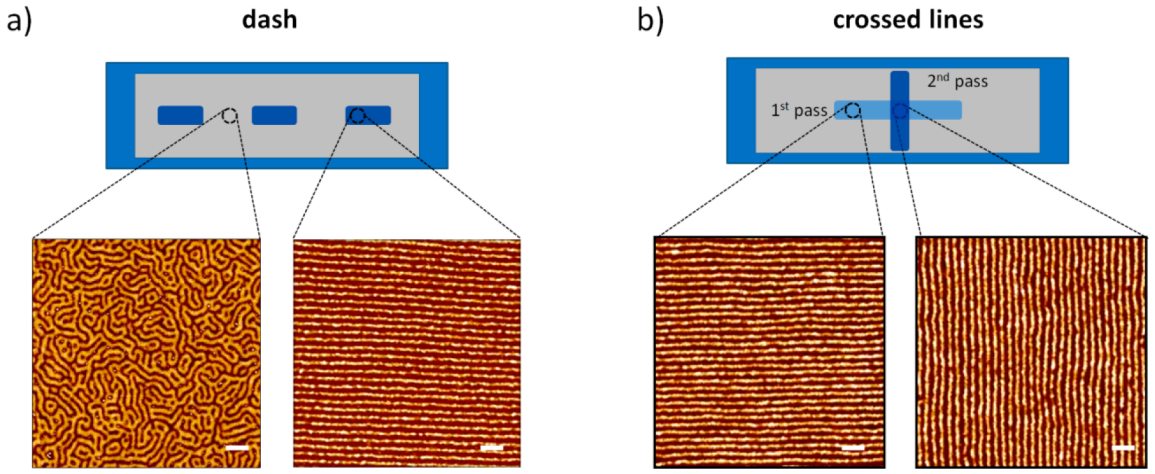

Figure 2. AFM phase images. (a) Dash pattern. The macroscopic dashes were spaced 5 mm apart, and the speeds for the "fast" and "slow" rastered regions were 100 and 10 μm/s, respectively. (b) Crossed line pattern. The SIS thin film was exposed to two orthogonal RSVA-SS linear pattern steps. Scale bars represent 100 nm for all AFM images.

Figure 1(b–d) presents the results of single RSVA-SS passes that were horizontal, vertical, and diagonal to the rectangular PDMS pad (a typical dimension of PDMS pad was 20 mm × 10 mm × 0.3 mm, rastering speed was 10 μm/s). The alignment of cylindrical domains in the SIS films was correlated strongly to the rastering direction instead of PDMS shape. This long-range ordering of SIS cylinders persisted across the entire area that was rastered by toluene vapor as determined through multiple AFM measurements across the surface. Although only the surface morphology was assessed in this study, the through-thickness nanostructure of films subjected to soft shear annealing has been investigated previously by grazing incidence small-angle X-ray scattering (GISAXS).[29] In that case, the soft shear process produced highly ordered cylindrical nanostructures over a range of film thickness (40 nm to 1 μm). Similar order through the thickness of the films is expected in this work, given that our film thickness is 90 nm and well within the range of the previous study.

The implementation of a solvent vapor delivery nozzle generated a localized (point) SVA zone in which both the PDMS and BP film were swollen by uptake of the solvent vapor, which plasticized the BP to enhance its mobility and enable domain ordering. Because the film was fixed to the substrate and moved with the motorized stage, an advancing swelling front and receding deswelling front were created. The swelling and deswelling of the PDMS pad produced a soft shear field to align the BP domains, similar in effect to CZA-SS in which shear force is obtained from the thermal expansion and contraction of PDMS. The rastering speed strongly impacted the solvent swelling and deswelling rates.[35] With the parameters employed in this work, highly oriented cylinders were produced with a rastering speed of 10 μm/s, and the SIS film retained its as-cast morphology with a rastering speed of 100 μm/s (see Supporting Information Figure S1). The width of the rastered area was approximately 4 mm for this particular setup with high pattern fidelity except as one approached the edge of the rastered zone (see Supporting Information Figure S2). Because the alignment quality correlates with the swollen ratio of the PDMS pad,[33] we note that films lose alignment at the end of the edge of the rastered region. At present, the lack of a step transition between highly aligned and unaligned structures at the edge of the rastered region is a potential shortcoming of RSVA-SS in comparison to graphoepitaxy or chemical prepatterning. The key process variables such as rastering speed, solvent flow rate, nozzle dimension, nozzle height, etc. are coupled in their influence on the solvent field and, ultimately, on the swelling ratio of the PDMS pad and the alignment quality of the SIS film. These parameters, together with the physical properties of the PDMS pad (e.g., cross-link density, thickness, etc.), will be investigated in detail in future studies.

A key feature of the RSVA-SS technique is the ability to produce complex patterns such as dashes, crossed lines, and curved structures as demonstrated in Figure 2 and Figure 3. First, a dash pattern was achieved by applying alternating slow and fast rastering speeds (10 versus 100 μm/s). The SIS

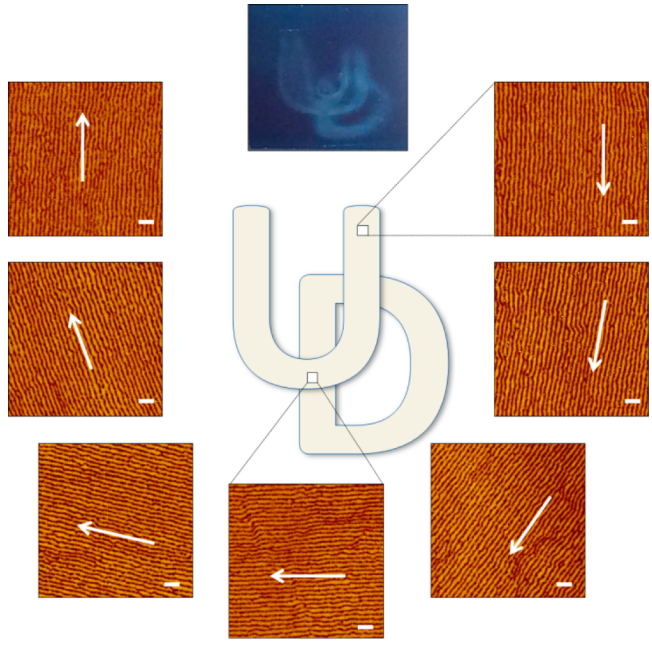

Figure 3. UD pattern. A UD pattern (top) was visible due to the shear effect (optical image with enhanced contrast). AFM phase images showed the SIS domains were aligned along the local shear direction. Arrows indicate direction of raster. Font size was 10 mm. Scale bars represent 100 nm for all AFM images.

DOI: 10.1021/acsmacrolett.5b00126
ACS Macro Lett. 2015, 4, 516–520

cylinders were strongly aligned in the "slow" rastered region, as compared to in the "fast" rastered region where the cylinders remained disordered due to low solvent uptake. The low uptake of solvent in the "fast" regions resulted in limited expansion and contraction of the PDMS pad and limited chain mobility in SIS (Figure 2a). The borders between the fast and slow rastered regions (poor alignment versus high alignment) were not as sharp as typically demonstrated by graphoepitaxy or chemical prepatterning. This alignment edge width in RSVA-SS may not be ideal for all applications, and combining RSVA-SS with other available tools might help improve the accuracy of the patterns.[27,31]

A second key feature, a crossed line pattern, was produced by rastering a line pattern, changing the raster direction, and rastering a second (orthogonal) line pattern. In this case, a new PDMS pad was used for each pass because the shape of the PDMS pad did not fully recover after deswelling. In Figure 2b, the alignment of the SIS cylinders was overridden by the second rastering pass in the coincident region, suggesting RSVA-SS can direct BP cylinders independent of any preexisting orientation, and a single BP thin film can be patterned multiple times. This facile, independent, and reusable patterning strategy is important for practical applications with BPs and, to our knowledge, is not achievable with other methods. We note that edge effects similar to those found in the dash pattern were present in the crossed line patterns as well, and the use of other available tools may lead to the potential fabrication of well-defined structures such as T-junctions and nanosquare arrays.[27,31]

We also show that the versatility of patterns could be achieved by using a two-dimensional motorized stage. Figure 3 displays a macroscopic "UD" pattern, which contained SIS cylinders that were microscopically aligned along the local shear direction. Again, this ability to "write" ordered BP nanostructures freely on pattern-free substrates based on the spatiotemporal swelling/deswelling of a PDMS pad offers unique advantages over conventionally patterning methods due to its simplicity and efficiency. The font size of the patterns could be tuned easily by the programmable stage and nozzle dimension, allowing controlled pattern formation in an on-demand fashion for practical use in various applications.

Furthermore, we demonstrate that the aligned BP pattern could be erased easily by a simple "bell jar" SVA treatment (Figure 4). Upon solvent removal from a film swollen to ~160% of the original film thickness, the film morphology was poorly ordered, similar to the as-cast morphology, and allowed for repatterning. We also note the nanopatterns could be erased locally by taking advantage of the RSVA process alone.[35] This erase and rewrite capability affords additional advantages over conventional patterning methods.

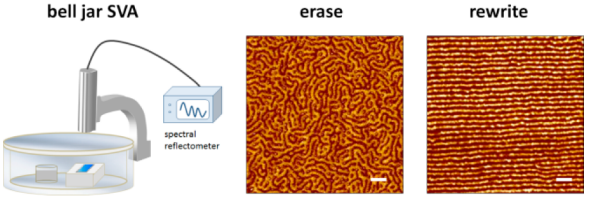

Figure 4. Erase–rewrite process. Aligned SIS domains became poorly ordered (middle AFM phase image) after a "bell jar" SVA treatment and were realigned by RSVA-SS (right AFM phase image). Scale bars represent 100 nm for all AFM images.

Another exciting aspect of RSVA-SS is its scalability for industrial production. For example, we fabricated a flat nozzle with a slit opening of dimension 5 cm × 1 mm (Figure 5). Two

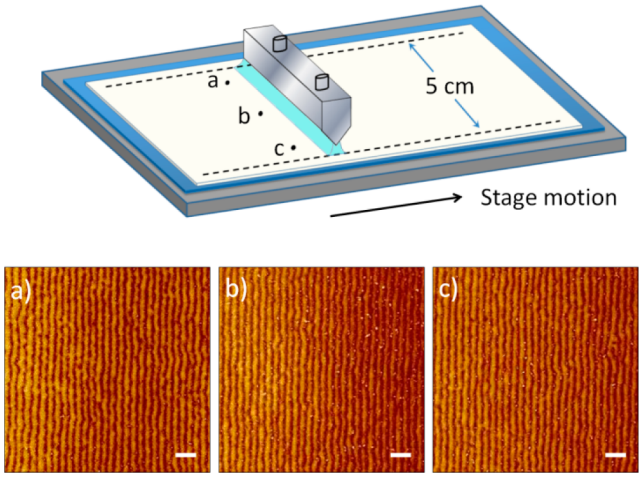

Figure 5. Large-scale production of highly ordered cylinders. AFM phase images of SIS thin film at different locations (a and c were 0.5 mm from the nozzle edge, b was in the center of the film) showed high quality of alignment in the rastering direction. Scale bars correspond to 100 nm.

inlets for solvent vapor stream, along with a graded opening, allowed the solvent to distribute uniformly through the thin slit. After the RSVA-SS process, multiple locations were examined by AFM and indicated a high degree of orientational ordering in the direction of the RSVA-SS, and this ordering persisted across the entire area exposed to the process. The RSVA-SS approach provides a feasible and scalable pathway to fabricate highly ordered BP cylinders at relatively high speed (mm/min) over unlimited dimensions.

In summary, we have developed a directed self-assembly method termed RSVA-SS to fabricate oriented BP cylinders on pattern-free substrates. The simplicity of the apparatus and the versatility of patterns possess advantages over other directed self-assembly methods, in particular with respect to a variety of polymers, patterns, and feature sizes. This unique ability to directly write macroscopic patterns with microscopically aligned BP nanostructures will unlock new avenues of applied research in nanotechnology and pave the way toward practical industrial use of hierarchically patterned BP nanostructures.

EXPERIMENTAL SECTION

Materials. Polystyrene-*b*-isoprene-*b*-styrene (SIS) with total molecular weight of 118 kg mol^{-1} and dispersity of 1.09 was obtained from DEXCO (V4211) and used as received. The volume composition for each block was f_S = 0.134, f_I = 0.732, and f_S = 0.134. In the bulk, the BP self-assembled into hexagonally packed polystyrene (PS) cylinders embedded in a polyisoprene (PI) matrix, with a nearest-neighbor spacing of 33 nm as determined from small-angle X-ray scattering. SIS films were flow coated onto the silicon substrates ($N\langle 100\rangle$, Wafer World, Inc.) from a 2.3 wt % solution of SIS in tetrahydrofuran. The film thickness was measured using a reflectance spectrometer (Filmetrics F20–UV). All the films used in this manuscript were ≈90 nm in thickness.

The elastomer pad was prepared from polydimethylsiloxane (PDMS, Dow Corning Sylgard 184) at 10:1 w/w ratio of base to curing agent and cured at 80 °C for 2 h. The thickness of the PDMS pad (approximately 0.3 mm) was controlled by spreading 1 g of PDMS in a Petri dish (2 in. in diameter).

DOI: 10.1021/acsmacrolett.5b00126
ACS Macro Lett. 2015, 4, 516–520

Raster Solvent Vapor Annealing and Shear Alignment. Raster solvent vapor annealing soft-shear (RSVA-SS) was performed using a setup in which 25 mL min^{-1} N_2 gas was bubbled through toluene to produce a solvent-rich vapor stream. The vapor stream was directed onto the film using a nozzle. As an example, the nozzle was constructed from a ground-flat 21-gauge hypodermic needle (0.514 mm inner diameter) attached to a vertical micrometer stage set 0.2 mm above the PDMS surface. The width of the rastered area was ≈4 mm and could be tuned by changing solvent flow rate, nozzle diameter, and needle height. The substrate-supported films were affixed to a programmable motorized stage to control the rastering speed and position. The rastering speed was 10 μm/s for the experiments performed in this manuscript, unless specified otherwise. The scale-up flat nozzle was custom-built using aluminum and had two inlets for solvent vapor (flow rate was 30 mL min^{-1} for each stream); the slit opening had a dimension of 5 cm × 1 mm.

Characterization. Atomic force microscopy (AFM) phase images were obtained on a Bruker Veeco Dimension 3100 with Nanoscope V controller operating in tapping mode using Budget Sensors TAP150-G tips (150 kHz, 5 N m^{-1}). Images were taken in the center of the rastered area along the rastering direction, but we note that the quality of alignment/orientation did not degrade until the very edge of the rastered area.

■ ASSOCIATED CONTENT

Supporting Information

Comparison of alignment quality at different rastering speeds. Comparison of alignment near the edge versus center of the rastered area. This material is available free of charge via the Internet at http://pubs.acs.org.

■ AUTHOR INFORMATION

Corresponding Author

*E-mail: thepps@udel.edu.

Notes

The authors declare no competing financial interest.

■ ACKNOWLEDGMENTS

We acknowledge support from NSF DMR-1207041. We thank the W. M. Keck Electron Microscopy Facility at the University of Delaware for use of the AFM instrument. We also thank Alfred Lance and Jeffrey Ricketts in the Chemical & Biomolecular Engineering Machine Shop for help with the design and fabrication of the scaled-up nozzle.

■ REFERENCES

(1) Park, S.; Lee, D. H.; Xu, J.; Kim, B.; Hong, S. W.; Jeong, U.; Xu, T.; Russell, T. P. *Science* **2009**, *323* (5917), 1030−1033.

(2) Yang, S. Y.; Ryu, I.; Kim, H. Y.; Kim, J. K.; Jang, S. K.; Russell, T. P. *Adv. Mater.* **2006**, *18* (6), 709−712.

(3) Bang, J.; Kim, S. H.; Drockenmuller, E.; Misner, M. J.; Russell, T. P.; Hawker, C. J. *J. Am. Chem. Soc.* **2006**, *128* (23), 7622−7629.

(4) Zschech, D.; Kim, D. H.; Milenin, A. P.; Scholz, R.; Hillebrand, R.; Hawker, C. J.; Russell, T. P.; Steinhart, M.; Gösele, U. *Nano Lett.* **2007**, *7* (6), 1516−1520.

(5) Ruiz, R.; Kang, H.; Detcheverry, F. A.; Dobisz, E.; Kercher, D. S.; Albrecht, T. R.; de Pablo, J. J.; Nealey, P. F. *Science* **2008**, *321* (5891), 936−939.

(6) Young, W.-S.; Kuan, W.-F.; Epps, T. H., III. *J. Polym. Sci., Part B: Polym. Phys.* **2014**, *52* (1), 1−16.

(7) Ruzette, A.-V. G.; Soo, P. P.; Sadoway, D. R.; Mayes, A. M. *J. Electrochem. Soc.* **2001**, *148* (6), A537−A543.

(8) Bates, C. M.; Maher, M. J.; Janes, D. W.; Ellison, C. J.; Willson, C. G. *Macromolecules* **2013**, *47* (1), 2−12.

(9) Guarini, K. W.; Black, C. T.; Zhang, Y.; Kim, H.; Sikorski, E. M.; Babich, I. V. *J. Vac. Sci. Technol. B* **2002**, *20* (6), 2788−2792.

(10) Park, M.; Chaikin, P. M.; Register, R. A.; Adamson, D. H. *Appl. Phys. Lett.* **2001**, *79* (2), 257−259.

(11) Chai, J.; Buriak, J. M. *ACS Nano* **2008**, *2* (3), 489−501.

(12) Black, C. T. *Appl. Phys. Lett.* **2005**, *87* (16), 163116.

(13) Terris, B. D.; Thomson, T. *J. Phys. D: Appl. Phys.* **2005**, *38* (12), R199.

(14) Luo, M.; Epps, T. H., III. *Macromolecules* **2013**, *46* (19), 7567−7579.

(15) Mishra, V.; Fredrickson, G. H.; Kramer, E. J. *ACS Nano* **2012**, *6* (3), 2629−2641.

(16) Albert, J. N. L.; Epps, T. H., III. *Mater. Today* **2010**, *13* (6), 24−33.

(17) Segalman, R. A.; Yokoyama, H.; Kramer, E. J. *Adv. Mater.* **2001**, *13* (15), 1152−1155.

(18) Bang, J.; Jeong, U.; Ryu, D. Y.; Russell, T. P.; Hawker, C. J. *Adv. Mater.* **2009**, *21* (47), 4769−4792.

(19) Kim, S. O.; Solak, H. H.; Stoykovich, M. P.; Ferrier, N. J.; de Pablo, J. J.; Nealey, P. F. *Nature* **2003**, *424* (6947), 411−414.

(20) Stoykovich, M. P.; Kang, H.; Daoulas, K. C.; Liu, G.; Liu, C.-C.; de Pablo, J. J.; Müller, M.; Nealey, P. F. *ACS Nano* **2007**, *1* (3), 168−175.

(21) Olszowka, V.; Tsarkova, L.; Boker, A. *Soft Matter* **2009**, *5* (4), 812−819.

(22) Majewski, P. W.; Gopinadhan, M.; Osuji, C. O. *J. Polym. Sci., Part B: Polym. Phys.* **2012**, *50* (1), 2−8.

(23) Yu, H.; Iyoda, T.; Ikeda, T. *J. Am. Chem. Soc.* **2006**, *128* (34), 11010−11011.

(24) Winey, K. I.; Patel, S. S.; Larson, R. G.; Watanabe, H. *Macromolecules* **1993**, *26* (16), 4373−4375.

(25) Young, W. S.; Epps, T. H., III. *Macromolecules* **2012**, *45* (11), 4689−4697.

(26) Angelescu, D. E.; Waller, J. H.; Adamson, D. H.; Deshpande, P.; Chou, S. Y.; Register, R. A.; Chaikin, P. M. *Adv. Mater.* **2004**, *16* (19), 1736−1740.

(27) Kim, S. Y.; Nunns, A.; Gwyther, J.; Davis, R. L.; Manners, I.; Chaikin, P. M.; Register, R. A. *Nano Lett.* **2014**, *14* (10), 5698−5705.

(28) Singh, G.; Yager, K. G.; Berry, B.; Kim, H.-C.; Karim, A. *ACS Nano* **2012**, *6* (11), 10335−10342.

(29) Qiang, Z.; Zhang, L.; Stein, G. E.; Cavicchi, K. A.; Vogt, B. D. *Macromolecules* **2014**, *47* (3), 1109−1116.

(30) Berry, B. C.; Bosse, A. W.; Douglas, J. F.; Jones, R. L.; Karim, A. *Nano Lett.* **2007**, *7* (9), 2789−2794.

(31) Jeong, J. W.; Hur, Y. H.; Kim, H.-j.; Kim, J. M.; Park, W. I.; Kim, M. J.; Kim, B. J.; Jung, Y. S. *ACS Nano* **2013**, *7* (8), 6747−6757.

(32) Sinturel, C.; Vayer, M.; Morris, M.; Hillmyer, M. A. *Macromolecules* **2013**, *46* (14), 5399−5415.

(33) Qiang, Z.; Zhang, Y.; Groff, J. A.; Cavicchi, K. A.; Vogt, B. D. *Soft Matter* **2014**, *10* (32), 6068−6076.

(34) Qiang, Z.; Zhang, Y.; Wang, Y.; Bhaway, S. M.; Cavicchi, K. A.; Vogt, B. D. *Carbon* **2015**, *82* (0), 51−59.

(35) Seppala, J. E.; Lewis, R. L., III; Epps, T. H., III. *ACS Nano* **2012**, *6* (11), 9855−9862.

DOI: 10.1021/acsmacrolett.5b00126
ACS Macro Lett. 2015, 4, 516−520